Repulsion of random and self-avoiding walks from excluded points and lines

1989 J. Phys. A: Math. Gen. 22 1621

(http://iopscience.iop.org/0305-4470/22/10/017)

J. Phys. A: Math. Gen. 22 (1989) 1621-1638. Printed in the UK

Repulsion of random and self-avoiding walks from excluded points and lines

D Considine and S Redner

Center for Polymer Studies and Department of Physics, Boston University, Boston MA 02215, USA

Received 21 September 1988, in final form 22 December 1988

Abstract. We investigate the repulsion of random walks (RWs) and self-avoiding walks (SAWs) induced by (*a*) excluding a single lattice point or (*b*) excluding all points on a half-line from $-\infty$ to the origin. For SAWs, we use exact enumeration and Monte Carlo methods to study the asymptotic behaviour of the displacement away from the excluded set on three-, four- and five-dimensional hypercubic lattices. When the SAW begins one lattice site away from an excluded point along the x direction, the mean displacement after N steps, $\langle x_N \rangle$ approaches a finite limit, at a power-law rate, as $N \to \infty$. However, the distribution of projected displacements exhibits a residual asymmetry in the asymptotic limit, reflective of a long-range influence of the excluded point. This general pattern of behaviour also occurs for a purely random walk. For a SAW which starts one lattice spacing away from the axis of the excluded half-line, enumeration data suggest that the mean displacement along the axis diverges as N^{ν}, with $\nu = \frac{3}{4}$ in two dimensions, but as N^{z}, with $z \simeq 0.35$, in three dimensions. This unexpected behaviour appears to be corroborated by constant-fugacity Monte Carlo data. However, for the corresponding RW model, both the solution to the diffusion equation and a heuristic argument indicate that $\langle x_N \rangle$ diverges as $N^{1/2}$ in two dimensions, and as $N^{1/2}/\ln N$ in three dimensions. Large values of N are needed before indications of this asymptotic behaviour are seen numerically. Similar crossover effects may be masking the asymptotic behaviour in the SAW problem.

1. Introduction

In this paper, we investigate the repulsion of random walks (RWs) and self-avoiding walks (SAWs) from a single excluded point, and from an excluded half-line (figure 1). That is, the random walk is absorbed if it touches the excluded set, and we study the statistical properties of the untrapped walkers. This work is motivated by previous studies which have shown that for RWs or SAWs in two dimensions, the mean displacement away from an excluded point, $\langle x_N \rangle$, increases logarithmically in the number of steps, N [1, 2]. These intriguing results lead us to undertake a more comprehensive investigation of the repulsion phenomenon, both as a function of the spatial dimension d, and as a function of the spatial extent of the excluded set.

For random walks originating one lattice spacing away from an excluded point, Weiss [1] used generating function methods to calculate the mean longitudinal displacement after N steps, $\langle x_N \rangle$. It was found that $\langle x_N \rangle \sim N^{1/2}$ for spatial dimension $d = 1$, $\langle x_N \rangle \sim \ln N$ for $d = 2$, while in higher dimensions, $\langle x_N \rangle$ asymptotically saturates at a finite value. This pattern of behaviour as a function of d stems from the transition between transience and recurrence of random walks [3-5]. For $d \leq 2$, a random walker

0305-4470/89/101621+18$02.50

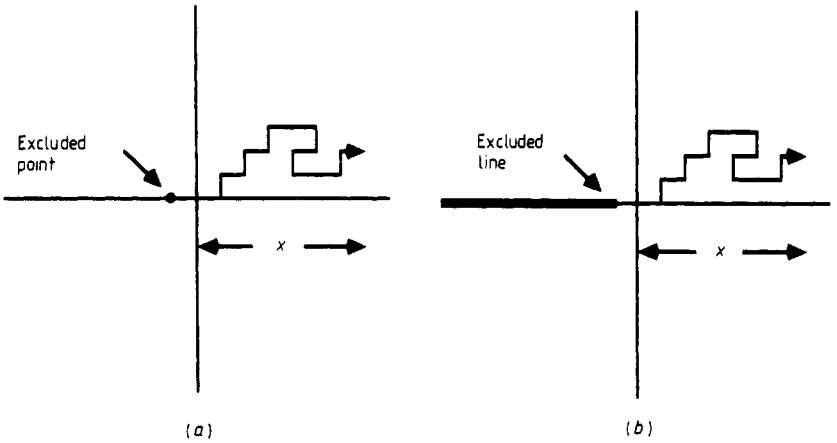

Figure 1. A random or self-avoiding walk in the presence of (*a*) an excluded point and (*b*) an excluded half-line. The average endpoint displacement and higher moments along the x axis are measured.

is certain to visit any lattice site, so that if a particular site is excluded, the walks which do not touch this site must necessarily be repelled by it. On the other hand for $d > 2$, the probability of eventually hitting any site is less than unity, so that the exclusion of one site does not lead to long-range repulsion.

For SAWs, the excluded site constraint is equivalent to fixing the direction of the first step, and the latter formulation is also known as the 'persistence' problem [2, 6, 7]. From this viewpoint, a basic question is how the initial directional bias is 'remembered' by the walk. For SAWs in two dimensions, it appears that $\langle x_N \rangle \sim \ln N$, while the higher odd moments, $\langle x_N^{2k+1} \rangle$, scale as $N^{2k\nu} \ln N$. This behaviour arises from a distribution of projected displacements whose antisymmetric component is of the form [2]: $A(x) \sim N^{-2\nu} \ln N \exp(-bx/N^{\nu})$.

In this work, we find that for SAW in the presence of an excluded point the repulsion weakens as the spatial dimension increases, as might be expected intuitively. Enumeration data indicate that $\langle x_N \rangle$ approaches a finite dimension-dependent 'presistence length', λ, as $N \to \infty$, and that $\langle x_N^{2k+1} \rangle$ scales as $N^{2k\nu}$. Such a pattern of behaviour could arise by shifting the unperturbed SAW displacement distribution by the finite value of the persistence length. However, this trivial construction does not account for the divergence of the higher odd cumulants of the displacement distribution as $N \to \infty$—behaviour which is indicative of a distribution whose approach to symmetry about λ is anomalously slow.

More interesting behaviour occurs when the repulsion effect is stronger, as embodied by the excluded needle problem. For a walk which begins one lattice spacing away along the axis of the needle, the higher moments of the endpoint distribution, projected along the needle axis, $\langle x_N^{2k+1} \rangle$, appear to diverge as $N^{(2k+1)\nu}$ in $d = 2$, where $\nu = \frac{3}{4}$ is the correlation length exponent of two-dimensional SAWs. Thus the walk is repelled from the needle at the same rate at which the distribution spreads out. In $d = 3$, our enumeration data suggests that $\langle x_N^{2k+1} \rangle \sim N^{2k\nu+z}$ for $k \geq 0$, with $z \simeq 0.35$. This unusual behaviour in which an apparent new exponent appears is also supported by constant-fugacity Monte Carlo simulations. This approach indicates that the antisymmetric component of the distribution of endpoint displacements, projected along the needle axis, is quite accurately fitted by the exponential form $A(x) \sim \bar{N}^{z-2\nu} \exp[-bx/\bar{N}^{\nu}]$,

where $\bar{N}$ is the average value of the number of steps in the walk at a fixed value of the fugacity per step, and b is a constant.

The potential existence of a new exponent leads us to study the corresponding problem of a RW in the presence of an excluded needle, both analytically and numerically. For the excluded needle, we give a heuristic argument which suggests that $\langle x_N \rangle$ diverges as $N^{1/2}$ in $d=2$, and as $N^{1/2}/\ln N$ in $d=3$. For the more general case of a diffusing particle exterior to an excluded wedge (cone for $d=3$) of arbitrary opening angle θ_0, the solution to the corresponding diffusion equation shows that the survival probability depends on θ_0, but that that $\langle x_N \rangle \sim A(\theta_0) N^{1/2}$. The amplitude $A(\theta_0)$ is a smooth, non-singular function of θ_0 in two dimensions, but in three dimensions $A(\theta_0)$ vanishes logarithmically in θ_0 in the excluded needle limit. This asymptotic behaviour is not manifested in the numerical data until relatively large N ($N \simeq 25$ and $N \geqslant 100$, respectively, for $d=2$ and 3). This slow crossover casts doubt on the aforementioned SAW results, which are based on relatively short series.

We first outline some new features of our enumeration method in § 2, and present data and analysis for SAWs in the presence of an excluded point and an excluded needle in §§ 3 and 4. We also describe and analyse Monte Carlo simulations which support the enumeration results for three-dimensional SAWs in the presence of an excluded needle. In § 5, we present analytical results for the persistence of random walks with no immediate returns allowed, and for random walks in the presence of an excluded point and excluded needle. These results are compared with the behaviours found in the corresponding SAW problem. We summarise in § 6 and discuss our numerical results for SAWs in light of the slow approach to asymptotic behaviour found for RW models.

2. Enumeration data and analysis

We have enumerated SAWs in the presence of an excluded point, and in the presence of an excluded line on hypercubic lattices for $d=2$–5. We used a standard enumeration program [8, 9], augmented by two time-saving modifications, which we briefly outline, as they may be of general interest. First, as the spatial dimension increases, it becomes relatively more advantageous to classify SAWs according to symmetry to a larger number of steps. For example, when the first step of the walk is fixed, then on the simple cubic lattice, there are five two-step SAWs, only two of which are topologically distinct. At three and four steps, there are, respectively, 6 and 22 topologically distinct SAWs out of 25 and 121 possible walks. Thus by enumerating only those SAWs built from the 22 distinct four-step bases, one needs to enumerate only $\frac{2}{11} = 0.\overline{18}$ of all possible SAW. In four and five dimensions, this four-step classification leads to a savings factor of $\frac{23}{337} \simeq 0.068$, and $\frac{23}{721} \simeq 0.032$, respectively, compared with a program with no symmetry classification. This symmetry classification leads to an enumeration time for SAWs of fixed number of steps which increases relatively slowly with the spatial dimension. In principle, it is possible to enumerate 13- or 14-step SAWs in arbitrary dimension with little additional resources beyond those used for the lower-dimensional enumerations.

With this improvement, however, memory requirements now become a significant limiting factor, as our check for a self-intersection in an N-step SAW is based on storing a hypercube of linear dimension $2N$. This requirement can be reduced by shifting the origin of each SAW so that the fifth step of the walk (which is the starting point of the enumeration in a four-step classification scheme) begins at the centre of the hypercube. By this device, a hypercube of linear dimension $2(N-4)$ needs to be stored for

Table 1. Enumeration data for the first three odd moments of the distribution of endpoint displacements along the x axis, for SAWs on hypercubic lattices, when the walk starts at the origin with an excluded site at $x = -1$.

N	$\langle x_N \rangle$	$\langle x_N^3 \rangle$	$\langle x_N^5 \rangle$
	Three dimensions		
1	0.200 00d +00	0.200 00d +00	0.200 00d +00
2	0.240 00d +00	0.480 00d +00	0.144 00d +01
3	0.289 26d +00	0.884 30d +00	0.425 62d +01
4	0.298 81d +00	0.133 79d +01	0.916 13d +01
5	0.323 64d +00	0.187 20d +01	0.167 86d +02
6	0.328 05d +00	0.243 13d +01	0.273 69d +02
7	0.342 39d +00	0.305 12d +01	0.415 86d +02
8	0.345 02d +00	0.368 51d +01	0.594 50d +02
9	0.354 38d +00	0.436 79d +01	0.817 01d +02
10	0.356 23d +00	0.505 98d +01	0.108 17d +03
11	0.362 85d +00	0.579 26d +01	0.139 68d +03
12	0.364 23d +00	0.653 15d +01	0.175 89d +03
13	0.369 19d +00	0.730 57d +01	0.217 71d +03
14	0.370 28d +00	0.808 42d +01	0.264 67d +03
15	0.374 12d +00	0.889 37d +01	0.317 74d +03
16	0.375 01d +00	0.970 62d +01	0.376 35d +03
17	0.378 09d +00	0.105 47d +02	0.441 52d +03
	Four dimensions		
1	0.142 86d +00	0.142 86d +00	0.142 86d +00
2	0.163 27d +00	0.285 71d +00	0.775 51d +00
3	0.186 94d +00	0.471 81d +00	0.196 74d +01
4	0.190 27d +00	0.665 52d +00	0.380 63d +01
5	0.200 00d +00	0.880 21d +00	0.638 69d +01
6	0.201 20d +00	0.109 76d +01	0.973 64d +01
7	0.206 48d +00	0.132 84d +01	0.139 44d +02
8	0.207 13d +00	0.156 03d +01	0.190 02d +02
9	0.210 36d +00	0.180 17d +01	0.249 98d +02
10	0.210 77d +00	0.204 37d +01	0.319 03d +02
11	0.212 93d +00	0.229 28d +01	0.398 05d +02
12	0.213 22d +00	0.254 22d +01	0.486 61d +02
13	0.214 75d +00	0.279 72d +01	0.585 61d +02
14	0.214 96d +00	0.305 25d +01	0.694 52d +02
	Five dimensions		
1	0.111 11d +00	0.111 11d +00	0.111 11d +00
2	0.112 35d +00	0.197 53d +00	0.493 83d +00
3	0.113 73d +00	0.303 74d +00	0.113 59d +01
4	0.113 88d +00	0.409 65d +00	0.205 32d +01
5	0.114 36d +00	0.523 57d +00	0.326 60d +01
6	0.114 40d +00	0.637 19d +00	0.477 79d +01
7	0.114 63d +00	0.755 15d +00	0.660 74d +01
8	0.114 65d +00	0.872 87d +00	0.875 11d +01
9	0.114 79d +00	0.993 34d +00	0.112 26d +02
10	0.114 80d +00	0.111 36d +01	0.140 25d +02
11	0.114 88d +00	0.123 58d +01	0.171 64d +02
12	0.114 89d +00	0.135 78d +01	0.206 34d +02
13	0.114 95d +00	0.148 13d +01	0.244 51d +02

Table 2. Enumeration data for the first three odd moments of the distribution of endpoint displacements along the x axis, for SAWs on the square, simple cubic and hypercubic lattices, when the half-line from $-\infty$ to the origin is excluded, and the walker starts from the origin.

N	$\langle x_N \rangle$	$\langle x_N^3 \rangle$	$\langle x_N^5 \rangle$
	Two dimensions		
1	0.333 33d + 00	0.333 33d + 00	0.333 33d + 00
2	0.444 44d + 00	0.111 11d + 01	0.377 78d + 01
3	0.600 00d + 00	0.252 00d + 01	0.150 00d + 02
4	0.724 64d + 00	0.472 46d + 01	0.415 94d + 02
5	0.841 27d + 00	0.769 84d + 01	0.941 74d + 02
6	0.943 69d + 00	0.114 64d + 02	0.184 50d + 03
7	0.105 02d + 01	0.160 87d + 02	0.326 90d + 03
8	0.114 89d + 01	0.216 00d + 02	0.537 41d + 03
9	0.124 72d + 01	0.280 17d + 02	0.834 02d + 03
10	0.134 04d + 01	0.353 67d + 02	0.123 64d + 04
11	0.143 29d + 01	0.436 63d + 02	0.176 56d + 04
12	0.152 25d + 01	0.529 47d + 02	0.244 51d + 04
13	0.161 08d + 01	0.632 11d + 02	0.329 85d + 04
14	0.169 70d + 01	0.745 05d + 02	0.435 33d + 04
15	0.178 19d + 01	0.868 12d + 02	0.563 54d + 04
16	0.186 53d + 01	0.100 19d + 03	0.717 61d + 04
17	0.194 75d + 01	0.114 61d + 03	0.900 32d + 04
18	0.202 85d + 01	0.130 13d + 03	0.111 52d + 05
19	0.210 84d + 01	0.146 72d + 03	0.136 52d + 05
20	0.218 72d + 01	0.164 44d + 03	0.165 44d + 05
21	0.226 51d + 01	0.183 26d + 03	0.198 57d + 05
22	0.234 21d + 01	0.203 25d + 03	0.236 36d + 05
23	0.241 81d + 01	0.224 35d + 03	0.279 13d + 05
24	0.249 35d + 01	0.246 64d + 03	0.327 35d + 05
	Three dimensions		
1	0.200 00d + 00	0.200 00d + 00	0.200 00d + 00
2	0.240 00d + 00	0.480 00d + 00	0.144 00d + 01
3	0.289 26d + 00	0.884 30d + 00	0.425 62d + 01
4	0.314 53d + 00	0.140 17d + 01	0.944 27d + 01
5	0.343 09d + 00	0.199 68d + 01	0.177 36d + 02
6	0.365 36d + 00	0.268 18d + 01	0.297 15d + 02
7	0.387 30d + 00	0.344 13d + 01	0.461 57d + 02
8	0.405 51d + 00	0.427 10d + 01	0.676 41d + 02
9	0.423 57d + 00	0.516 48d + 01	0.947 83d + 02
10	0.439 34d + 00	0.612 15d + 01	0.128 18d + 03
11	0.454 90d + 00	0.713 57d + 01	0.168 39d + 03
12	0.468 95d + 00	0.820 72d + 01	0.216 01d + 03
13	0.482 75d + 00	0.933 15d + 01	0.271 54d + 03
14	0.495 46d + 00	0.105 09d + 02	0.335 57d + 03
15	0.507 93d + 00	0.117 35d + 02	0.408 57d + 03
16	0.519 56d + 00	0.130 10d + 02	0.491 11d + 03
17	0.531 00d + 00	0.143 31d + 02	0.583 64d + 03
	Four dimensions		
1	0.142 86d + 00	0.142 86d + 00	0.142 86d + 00
2	0.163 27d + 00	0.285 71d + 00	0.775 51d + 00

Table 2. (continued)

Four dimensions			
N	$\langle x_N \rangle$	$\langle x_N^3 \rangle$	$\langle x_N^5 \rangle$
3	0.186 94*d* + 00	0.471 81*d* + 00	0.196 74*d* + 01
4	0.195 94*d* + 00	0.687 96*d* + 00	0.389 90*d* + 01
5	0.206 59*d* + 00	0.918 12*d* + 00	0.664 83*d* + 01
6	0.213 11*d* + 00	0.116 71*d* + 01	0.102 87*d* + 02
7	0.219 99*d* + 00	0.142 71*d* + 01	0.149 17*d* + 02
8	0.225 10*d* + 00	0.169 97*d* + 01	0.205 76*d* + 02
9	0.230 24*d* + 00	0.198 15*d* + 01	0.273 39*d* + 02
10	0.234 34*d* + 00	0.227 25*d* + 01	0.352 46*d* + 02
11	0.238 42*d* + 00	0.257 12*d* + 01	0.443 47*d* + 02
12	0.241 82*d* + 00	0.287 72*d* + 01	0.546 79*d* + 02
13	0.245 20*d* + 00	0.318 96*d* + 01	0.662 84*d* + 02
Five dimensions			
1	0.111 11*d* + 00	0.111 11*d* + 00	0.111 11*d* + 00
2	0.123 45*d* + 00	0.197 53*d* + 00	0.493 83*d* + 00
3	0.137 31*d* + 00	0.303 74*d* + 00	0.113 59*d* + 01
4	0.141 50*d* + 00	0.420 13*d* + 00	0.209 57*d* + 01
5	0.146 57*d* + 00	0.539 69*d* + 00	0.336 98*d* + 01
6	0.149 11*d* + 00	0.664 82*d* + 00	0.497 65*d* + 01
7	0.151 90*d* + 00	0.791 86*d* + 00	0.693 20*d* + 01
8	0.153 65*d* + 00	0.921 94*d* + 00	0.923 82*d* + 01
9	0.155 49*d* + 00	0.105 36*d* + 01	0.119 10*d* + 02
10	0.156 78*d* + 00	0.118 72*d* + 01	0.149 48*d* + 02
11	0.158 11*d* + 00	0.132 21*d* + 01	0.183 62*d* + 02
12	0.159 11*d* + 00	0.145 83*d* + 01	0.221 54*d* + 02
13	0.160 13*d* + 00	0.159 55*d* + 01	0.263 30*d* + 02

performing the self-intersection check. A further saving of memory is possible by storing a hyperdiamond rather than a hypercube, thereby eliminating inaccessible corners, but we did not pursue this option.

A second noteworthy point is that most of the time in the enumeration is spent in constructing the last step in the walk; this is especially true in higher dimensions. Thus improvements in the efficiency of this small portion of the code will reap significant savings in computer time. Our approach is based on 'unrolling' the last (or last two) do-loops implicit in the enumeration algorithm. It is then possible to count the number of N-step (or $(N-1)$-step) SAWs with arithmetic statements only, rather than using the conditional statements that the algorithm normally employs to build each step of a SAW. By this technique, the computer time needed to enumerate N-step walks is, in general, only marginally longer than the time needed to enumerate $(N-1)$-step walks, when the unrolling device is not employed.

With an excluded point, we obtained the distribution of endpoint displacements, projected along the direction of the first step, $P_N(x)$, for $N \leq 17$, 14 and 13, for $d = 3$, 4 and 5, respectively. These enumerations required approximately 12.5, 16 and 19.5 hours of CPU time on an IBM 3090 computer. Similarly, for the excluded needle problem, we obtained the distribution of endpoint displacements, projected along the needle axis, for $N \leq 24$, 17, 13 and 13 steps for $d = 2$, 3, 4 and 5, respectively. The first three odd moments of these two distributions are given in tables 1 and 2.

3. SAWs in the presence of an excluded point

The data of table 1 illustrate that the first moments of the displacement distribution grow very slowly with N, while the higher odd moments increase at a much faster rate. Using a variety of analysis methods, $\langle x_N \rangle$ can be well fitted by the form

$$\langle x_N \rangle = \lambda(1 - AN^{-\Delta}) \tag{1}$$

where λ and A are lattice- and dimension-dependent constants, and where we expect that Δ will depend only on the spatial dimension (table 3). Our result for the first moment in three dimensions is in agreement with earlier work by Grassberger [6].

In contrast, the higher odd moments appear to follow the power-law form

$$\langle x_N^{2k+1} \rangle \sim N^{2k\nu}. \tag{2}$$

This qualitatively parallels the behaviour found for two-dimensional SAW, except for the absence of logarithmic factors. To test the validity of (2), we studied the ratios

$$r_N(k) \equiv \frac{\langle x_N^{2k+1} \rangle}{\langle x_N^2 \rangle^k}. \tag{3}$$

According to (2), the numerator has the same asymptotic behaviour as the denominator, and $r_N(k)$ should approach a constant as $N \to \infty$. As a function of N, we find that $r_N(k)$ is a weakly increasing sequence, whose rate of increase slows for larger values of N. Series analysis indicates that this rate of growth is slower than a power law in N, and on this basis, it appears that $\langle x_N^{2k+1} \rangle \sim \langle x_N^2 \rangle^k \sim N^{2k\nu}$, asymptotically, with no logarithmic factors present, as in the two-dimensional case, although appreciable non-asymptotic corrections do exist.

Table 3. Estimates of the values of A and Δ for SAWs with an excluded point, and the persistence lengths, λ, for SAWs, for random walks with no immediate returns (RWNR), and for random walks with an excluded point (RWEP).

			λ		
d	A	Δ	SAW	RWNR	RWEP
3	0.29 ± 0.04	0.76 ± 0.06	0.42 ± 0.01	$\frac{1}{4}$	0.516...
4	0.15 ± 0.03	1.05 ± 0.10	0.22 ± 0.01	$\frac{1}{6}$	0.25
5	0.11 ± 0.03	1.50 ± 0.10	0.15 ± 0.01	$\frac{1}{8}$	0.15

This pattern of behaviour for the moments could arise by shifting the unperturbed SAW endpoint displacement distribution by the persistence length. To test for this trivial possibility, we investigate the symmetry of the displacement distribution about the persistence length by studying the higher cumulants

$$\kappa_N(k) \equiv \langle (x_N - \langle x_N \rangle)^k \rangle \tag{4}$$

which would all vanish if the distribution were symmetric about $\langle x_N \rangle$. The data for $\kappa_N(k)$ suggest that they all diverge to $-\infty$ as $N \to \infty$, except in five dimensions, where $\kappa_N(k) \to +\infty$ for $k \geq 5$. The absence of perfect symmetry in the distribution in the asymptotic limit is indicative of vestiges of the initial bias in the walk. However, this divergence of the cumulants is sufficiently slow that the skewness of the distribution, $S = \kappa_N(3)/\kappa_N(2)^{3/2}$, still vanishes as $N \to \infty$. Thus the distribution asymptotically becomes symmetric, but only at a relatively slow rate.

4. SAWs in the presence of an excluded needle

The primary qualitative difference between the data for the excluded needle and excluded point geometries is that the first moment in the excluded needle problem increases more rapidly, and at a rate that is consistent with a power-law divergence. In two dimensions, straightforward analysis of the data indicates that $\langle x_N \rangle \sim N^{\nu}$, where $\nu = \frac{3}{4}$, and more generally, $\langle x_N^{2k+1} \rangle \sim N^{(2k+1)\nu}$. Thus the repulsion induced by the needle gives rise to a mean displacement which is as rapid as the spread of the probability distribution of an unperturbed SAW itself. In three dimensions, the situation is considerably more interesting (figure 2). Our Neville-table analysis indicates that $\langle x_N \rangle \sim N^{z}$, with $z \simeq 0.35$, while the higher odd moments appear to scale as $\langle x_N^{2k+1} \rangle \sim N^{z+2k\nu}$. Thus it appears that a new exponent, z, in addition to the correlation exponent ν, is needed to account for all the moments of the displacement distribution.

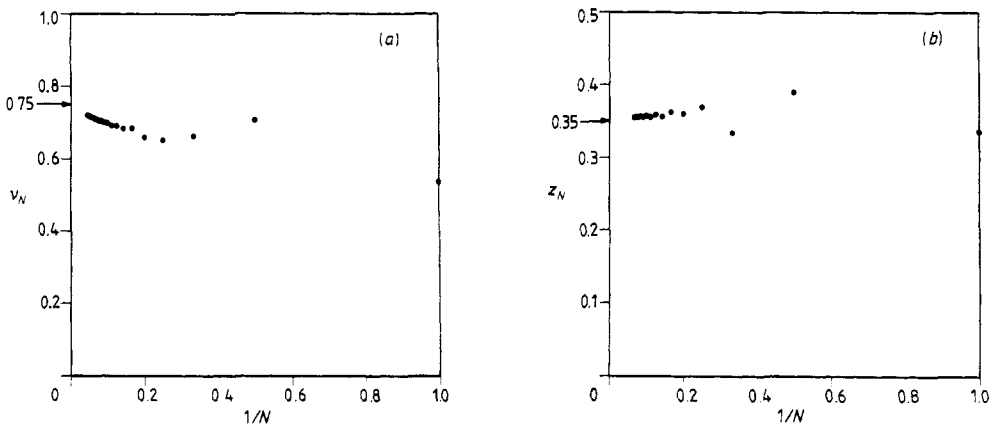

Figure 2. Enumeration results for SAWs in the presence of an excluded needle. Shown are the finite-N estimates for the exponents describing the divergence of the odd moments of the displacement distribution, plotted against $1/N$. The arrows show the estimates for the asymptotic values of the exponents based on Neville-table analysis.

To corroborate this unusual behaviour, we have also performed constant-fugacity Monte Carlo simulations for three-dimensional excluded needle geometry. The constant-fugacity method generates an unbiased ensemble of SAWs, in which each step of the walk has a fugacity per step, p, so that each N-step SAW has a relative weight of p^N. The average number of steps in the ensemble of walks, $\bar{N}(p)$, varies as $(p - p_c)^{-1}$, with $p_c = 1/\mu \simeq 0.2135$ [7]. We simulated extensively for p in the range 0.13–0.206, corresponding to $\bar{N}(p) \leqslant 32$. This simulation method is of sufficient accuracy that it can be used to effectively augment the enumeration data.

We measured the fugacity-dependent distribution of endpoint displacements, $P(x, p)$, projected along the axis of the needle. This distribution can be decomposed into a symmetric $S(x, p) = \frac{1}{2}[P(x, p) + P(-x, p)]$, and an antisymmetric component, $A(x, p) = \frac{1}{2}[P(x, p) - P(-x, p)]$, respectively, with the behaviour of the odd moments of the distribution being governed solely by $A(x, p)$. Figure 3 suggests that $A(x, p)$ is a pure exponential function

$$A(x, p) = A(p)\, \mathrm{e}^{-a(p)x}. \tag{5}$$

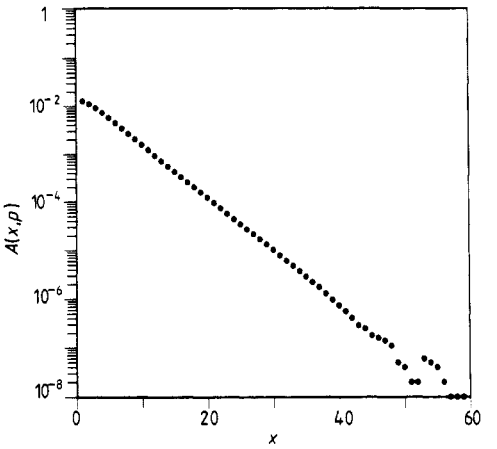

Figure 3. A semilogarithmic plot of the antisymmetric component of the displacement distribution at fugacity $p = 0.206$, corresponding to $\bar{N} \approx 32$.

This exponential behaviour was found previously in the case of 2D SAWs with the direction of the first step fixed [2], but with different scaling dependences of $A(p)$ and $a(p)$. By linear regression analysis, we find that $a(p) \sim \bar{N}^{-\nu}$, and $A(p) \sim \bar{N}^{z-2\nu}$ with ν the correlation length exponent, and $z \simeq 0.35$. Thus our analysis suggest that $A(x, p)$ has the form

$$A(x, p) \sim \bar{N}^{z-2\nu} \exp(-bx/\bar{N}^{\nu}) \tag{6}$$

where b is a constant.

These results for three-dimensional SAWs in the presence of an excluded needle are quite puzzling as there does not appear to be a physical mechanism that gives rise to a second independent length, in addition to the correlation length. We therefore turn to an analytical study of corresponding RW models in order to gain further insights. This study will suggest that the SAW results arise from a relatively slow crossover effect, so that there is no new exponent in the problem.

5. Analytical study of persistence in random walks

In order to have $\langle x_N \rangle \sim \mathcal{O}(1)$ and $\langle x_N^{2k+1} \rangle \sim N^{2k\nu}$, one can take a pure random walk, with the direction of the first step fixed along $+x$. Since each step of the walk is independent, the distribution of projected displacements is a symmetric Gaussian which is centred at $x = 1$. Consequently, $\langle x_N \rangle \equiv 1$, and $\langle x_N^{2k+1} \rangle \sim N^{2k\nu}$, with $\nu = \frac{1}{2}$. However, this trivial construction does not reproduce the observed asymmetry of the distribution about the persistence length for SAWs. More interesting behaviour is provided by the models of a random walk with no immediate returns allowed, and by

a random walk in the presence of an excluded point and an excluded line. In the first case, the mechanism for the persistence of the initial directional bias is local in character, as fixing the first step leads to a short-term memory effect. For the latter two models, the repulsion of the respective excluded sets is long-range in nature, and the resulting behaviour is useful in interpreting our results for the corresponding SAW models.

5.1. Random walk with no immediate reversals

For a random walk which is prohibited from immediately reversing direction at each step [10], we can compute the moments of the displacement distribution exactly. For this purpose, we only need to classify walks according to the number of steps in the $+x$ and $-x$ direction, and the number of steps in the remaining $2(d-1)$ transverse directions. Assigning fugacities r, l and t, respectively, for these three cases, then the statistical weight for all $(N+1)$-step walks, with the first step fixed in the $+x$ direction, is given by the matrix product

$$(1\ \ 1\ \ 1)\mathbf{T}^N\begin{pmatrix} r \\ 0 \\ 0 \end{pmatrix} \tag{7}$$

where $\mathbf{T}$ is the matrix

$$\begin{pmatrix} r & 0 & r \\ 0 & l & l \\ qt & qt & (q-1)t \end{pmatrix} \tag{8}$$

and $q=2(d-1)$. The generating function for all walks with the first step in the $+x$ direction is

$$G(r,l,t)=(1\ \ 1\ \ 1)(\mathbf{I}+\mathbf{T}+\mathbf{T}^2+\ldots)\begin{pmatrix} r \\ 0 \\ 0 \end{pmatrix}$$

$$=\frac{r\{(1-l)[1-(q-1)t]+qt(1-l)\}}{[1-(q-1)t](1-r)(1-l)-qt[r(1-l)+l(1-r)]}. \tag{9}$$

The generating function for the kth moment of the difference between the number of steps in the $+x$ and $-x$ directions,

$$\mathcal{N}_k(z)=\left(r\frac{\partial}{\partial r}-l\frac{\partial}{\partial l}\right)^k G(r,l,t)|_{r=l=t=z} \tag{10}$$

yields the moments of the displacement distribution via

$$\langle x_N^k\rangle=\frac{N\text{th term in the expansion of } \mathcal{N}_k(z)}{N\text{th term in the expansion of } G(z)}. \tag{11}$$

The terms in the series for $\langle x_N^k\rangle$ can be evaluated by direct power-series expansion of the generating functions, or by using contour integral techniques. For the first moment, we obtain

$$\langle x_N\rangle=\frac{1}{q}\left[1-\left(\frac{1}{1+q}\right)^N\right] \tag{12}$$

so that the persistence length $\lambda = 1/q$, is approached exponentially in N. The value of λ compares fairly well with the corresponding estimates for the SAW model, and the agreement improves as d is increased (table 3). However, the exponential form of the correction terms indicates that the memory of the initial step is lost considerably faster than in the SAW model.

Similar calculations yield $\langle x_N^{2k+1}\rangle \sim A(k, d)N^k$, with $A(k, d)$ depending on k and d, while the higher cumulants approach dimension-dependent constants as $N \to \infty$. This leads to the skewness of the distribution approaching zero as $N^{-3/2}$, which is faster than the rate at which the skewness vanishes for the corresponding SAW model. Thus the random walk with no immediate returns accounts for the asymptotic behaviour of the moments in the corresponding SAW problem, but not for the rate at which this asymptotic behaviour is attained. We attribute this discrepancy to the short-range nature of the correlations for this type of random walk.

5.2. Random walk with an excluded point

For RWs which start one lattice spacing from an excluded point, the moments of the displacement distribution can be calculated by the generating function formalism [1, 3-5]. Following Weiss [1], we study the behaviour of $U_N(\boldsymbol{r})$, the probability that a random walk is at $\boldsymbol{r}$ after N steps, when the lattice has a 'sticky' site at $\boldsymbol{s}$. This probability distribution obeys the recursion relations

$$U_{N+1}(\boldsymbol{r}) = \sum_{\boldsymbol{l}} U_N(\boldsymbol{l})p(\boldsymbol{r}-\boldsymbol{l}) - U_N(\boldsymbol{s})p(\boldsymbol{r}-\boldsymbol{s}) \tag{13}$$

$$U_{N+1}(\boldsymbol{s}) = \sum_{\boldsymbol{l}} U_N(\boldsymbol{l})p(\boldsymbol{s}-\boldsymbol{l}) + U_N(\boldsymbol{s}). \tag{14}$$

The second equality expresses the fact that if the walker reaches $\boldsymbol{s}$ it 'sticks' there permanently. In terms of the generating function

$$U(\theta, z) = \sum_{N=0}^{\infty} \sum_{\boldsymbol{r}} U_N(\boldsymbol{r}) z^N \, \mathrm{e}^{\mathrm{i}\boldsymbol{r}\cdot\theta} \tag{15}$$

the above recursion relations lead to

$$U(\theta, z) = \frac{1}{1 - z\lambda(\theta)} + \frac{F(\boldsymbol{s}, z)}{(1-z)}\left(1 - \frac{(1-z)}{(1 - z\lambda(\theta))}\right)\mathrm{e}^{\mathrm{i}\boldsymbol{s}\cdot\theta} \tag{16}$$

where $\lambda(\theta)$ is the structure function for the walk, and $F(\boldsymbol{s}, z)$ is the generating function for the first passage probability, $F_N(\boldsymbol{s})$, that the walk reaches $\boldsymbol{s}$ for the first time on step N.

The distribution of the subset of walks that remain untrapped at step N, $U'_N(\boldsymbol{r})$, is simply given by

$$U'_N(\boldsymbol{r}) = U_N(\boldsymbol{r}) - U_N(\boldsymbol{s})\delta_{\boldsymbol{r},\boldsymbol{s}} \tag{17}$$

i.e. the probability of being at $\boldsymbol{s}$ is subtracted from the probability distribution. The corresponding generating function can be written as [1]

$$U'(\theta, z) = \frac{1 - F(\boldsymbol{s}, z)\,\mathrm{e}^{\mathrm{i}\boldsymbol{s}\cdot\theta}}{1 - z\lambda(\theta)}. \tag{18}$$

For an excluded point located at $\boldsymbol{s} = (-1, 0, 0, \ldots)$, and with the random walk starting

at the origin, the moments of the displacement in the x direction can be obtained from,

$$\langle x_N^k \rangle = \frac{N\text{th term in the expression of } (-i\partial/\partial\theta_x)^k U'(\theta, z)|_{\theta=0}}{N\text{th term in the expansion of } U'(0, z)}. \tag{19}$$

From the asymptotic forms of $F(s, z)$, given by Lindenberg *et al* [11], we find that the mean displacement converges to a finite dimension-dependent value as $N \to \infty$:

$$\lambda = \frac{f_{sd}}{1 - f_{sd}} \tag{20}$$

where f_{sd} is the probability of ever reaching the point s in d dimensions. In three dimensions f_{sd} has been evaluated for several values of s [3], and the corresponding value of λ is given in table 3, along with approximate values in four and five dimensions. These persistence lengths agree quite closely with the corresponding values found in the SAW model, even in three dimensions, where excluded-volume effects are still relevant. Furthermore, the series for $\langle x_N \rangle$ approach their respective asymptotic values at a power-law rate, the higher odd moments scale as $\langle x_N^{2k+1} \rangle \sim N^k$, and the cumulants exhibit a pattern of behaviour which is similar to that of SAWs. Thus we conclude that the behaviour of SAWs and RWs in the presence of an excluded point is quite close.

5.3. Random walk with an excluded line

We now turn to the problem of a random walk in the presence of an excluded needle to compare with the results of the corresponding SAW model. We first compute the survival probability and the mean displacement from the solution to the diffusion equation with appropriate boundary conditions [12–14], and then provide heuristic arguments that lead to the same results.

In two dimensions, the diffusion equation is

$$\frac{1}{D}\frac{\partial P}{\partial t} = \frac{\partial^2 P}{\partial r^2} + \frac{1}{r}\frac{\partial P}{\partial r} + \frac{1}{r^2}\frac{\partial^2 P}{\partial \theta^2} \tag{21}$$

where $P = P(r, \theta, t)$ is the probability that a diffusing particle is at (r, θ, t), and D is the diffusion coefficient. We are interested in solving this equation subject to absorbing boundary conditions on the half-line $x < 0$, $y = 0$. This boundary condition accounts for the exclusion of the random walkers from the half-line. More generally, consider a wedge geometry (figure 4) of opening angle θ_0, which extends from $\theta = -\theta_0/2$ to

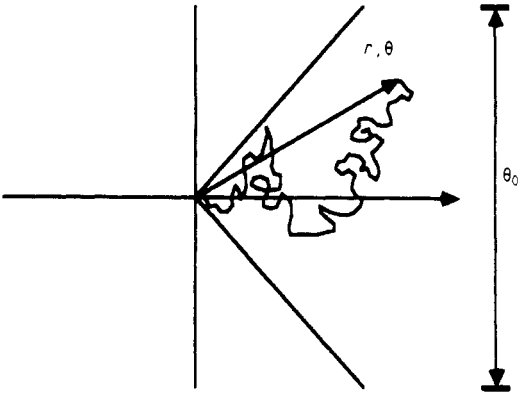

Figure 4. A random walk moving within an absorbing cone of opening angle θ_0.

$\theta = \theta_0/2$, with the boundary condition

$$P(r, \theta, t) = 0 \qquad \text{for} \qquad \theta = \pm\theta_0/2. \tag{22}$$

The excluded needle problem is the limiting case $\theta_0 = 2\pi$. Without loss of generality, we choose the initial condition

$$P(r, \theta, 0) = \delta(r - r')\delta(\theta). \tag{23}$$

To solve (21), we perform a Fourier transform on the variable θ in the finite range $|\theta| \leq \theta_0/2$, leading to

$$\frac{1}{D}\frac{\partial \bar{P}}{\partial t} = \frac{\partial^2 \bar{P}}{\partial r^2} + \frac{1}{r}\frac{\partial \bar{P}}{\partial r} - \frac{\nu^2}{r^2}\bar{P} \tag{24}$$

where $\bar{P}$ is the Fourier-transformed function, $\nu = (1+2n)\pi/\theta_0$, and n is a positive integer. Next we eliminate the radial variable, by introducing the Hankel transform [12],

$$H_\nu[v(r)] = \int_0^\infty rJ_\nu(\sigma r)v(r)\,\mathrm{d}r \tag{25}$$

and the corresponding inverse transform

$$v(r) = \int_0^\infty \sigma J_\nu(\sigma r)H_\nu\,\mathrm{d}\sigma. \tag{26}$$

Here $J_\nu(x)$ is the Bessel function of order ν. This transform has the property that

$$H_\nu\left(\frac{\partial^2 v}{\partial r^2} + \frac{1}{r}\frac{\partial v}{\partial r} - \frac{\nu^2}{r^2}v\right) = -\sigma^2 H_\nu(v). \tag{27}$$

The resulting first-order ordinary differential equation in time can then be solved straightforwardly, and the final solution is then obtained by inverse transforms. This procedure yields

$$P(r, \theta, t) = \left(\frac{r'}{\theta_0 Dt}\right)\exp\left(\frac{-(r^2+r'^2)}{4Dt}\right)\sum_\nu \cos(\nu\theta)I_\nu\left(\frac{rr'}{2Dt}\right) \tag{28}$$

where $I_\nu(z)$ is the modified Bessel function. For asymptotic behaviour, we consider only the lowest-order Bessel function in the limit of small argument. We find for $r \gg r'$,

$$P(r, \theta, t) \sim \frac{1}{t}\left(\frac{r}{t}\right)^{\pi/\theta_0}\exp\left(-\frac{r^2}{4Dt}\right)\cos\left(\frac{\pi\theta}{\theta_0}\right) \tag{29}$$

from which the survival probability, $S(t)$, and all the moments of the displacement along the wedge axis can be obtained. Integrating the above probability distribution over the accessible spatial region, gives $S(t) \sim t^{-\pi/2\theta_0}$. (This result can also be obtained by image methods when π/θ_0 is an integer.) Thus for $\theta_0 = 2\pi$, i.e. the excluded needle problem, $S(t)$ vanishes as $t^{-1/4}$. More interestingly, the mean displacement varies as $\langle x(t)\rangle \sim A(\theta_0)t^{1/2}$, with $A(\theta_0)$ a smooth non-singular function of θ_0. Thus the exponent in the time dependence of $\langle x(t)\rangle$ is *independent* of the opening angle of the wedge.

In three dimensions, the solution to the analogous excluded cone geometry, with the same initial and boundary conditions as in the two-dimensional problem, is given by Carslaw and Jaeger [12] in terms of a sum over the non-integral Legendre functions

$$P(r,\theta,t)=C\sum_{\nu}\exp\left(-\frac{(r^2+r'^2)}{4Dt}\right)(2\nu+1)I_{\nu}\left(\frac{rr'}{2Dt}\right)P_{\nu}(\mu) \tag{30}$$

where

$$C=-\left(\frac{1}{4\pi t(rr')^{1/2}}\right)\left[(1-\mu_0^2)\left(\frac{\partial}{\partial\mu_0}P_{\nu}(\mu_0)\right)\left(\frac{\partial}{\partial\nu}P_{\nu}(\mu_0)\right)\right]^{-1} \tag{31}$$

with $\mu=\cos\theta$ and $\mu_0=\cos(\theta_0/2)$. The summation is carried out over the non-integral set of ν values for which $P_{\nu}(\mu_0)=0$, thus satisfying the boundary conditions. Owing to a logarithmic divergence of $P_{\nu}(\mu_0)$ as $\mu_0\to-1$, we first consider θ_0 close to 2π, and then examine the limiting behaviour as $\mu_0\to-1$.

From (30), the survival probability is

$$S(t)\sim\frac{1}{t}\int_0^{\infty}dr\,r^{3/2}\exp\left(-\frac{(r^2+r'^2)}{4Dt}\right)I_{\nu_0+1/2}(z)\int_0^{\theta_0/2}P_{\nu_0}(\mu)\sin\theta\,d\theta. \tag{32}$$

where we have retained only the asymptotically dominant term with the lowest index of the Bessel function, ν_0, and $z=rr'/2Dt$. As in the two-dimensional case, the Bessel function can be approximated as $I_{\nu_0+1/2}(z)\sim z^{\nu_0+1/2}$ as $z\to0$, and the integral over the radial variable yields a factor of $t^{-\nu_0/2}$.

To perform the angular integral, note that for θ_0 close to 2π, the zeros of the Legendre function are very nearly integral, taking on values $\nu_s=s+\varepsilon_s$, where $s=0,1,2,\ldots$ [15]. The lowest zero has the value

$$\nu_0=\left[\ln\left(\frac{2}{1+\mu_0}\right)\right]^{-1} \tag{33}$$

while the corresponding lowest-order Legendre function has the approximate form [15, 16]

$$P_{\varepsilon_0}(\mu)\simeq1+\frac{\varepsilon_0\ln(\mu+1)}{2}. \tag{34}$$

That is, this function is nearly constant, except for a small conical region about the needle. Thus the integral over the angular variable approaches the value 2 as $\mu_0\to-1$, and we conclude that the survival probability in three dimensions scales as $t^{-\nu_0/2}$, with $\nu_0\to0$ as $\theta_0\to2\pi$.

The mean displacement can be calculated similarly, and we find $\langle x(t)\rangle\sim A(\theta_0)t^{1/2}$. However, in contrast with the two-dimensional case, $A(\theta_0)\sim[\ln(1+\mu_0)]^{-1}\to0$ as $\mu_0\to-1$. This singularity in the amplitude can be viewed as modifying the leading asymptotic behaviour of $\langle x(t)\rangle$ in the following sense. For a discrete random walk, the minimal lateral distance to the needle is one lattice spacing, and it therefore has an 'effective' opening angle which vanishes no faster than $N^{-1/2}$, where N is the number of steps in the walk. Employing this effective opening angle in the amplitude function $A(\theta_0)$, we find that it vanishes as $1/(\ln N)$. Thus this line of reasoning suggests that for a discrete random walk, $\langle x_N\rangle\sim N^{1/2}/\ln N$.

We now provide a qualitative argument which reproduces the results obtained from the solution to the diffusion equation. Our argument for the behaviour of the first

moment is based on the fact that if the excluded set is viewed as being 'sticky' rather than absorbing, then the mean displacement of all walks, both trapped and untrapped, is zero [1]. That is

$$p_{tr}(N)\langle x_{tr}(N)\rangle + p_{un}(N)\langle x_{un}(N)\rangle = 0 \tag{35}$$

or

$$\langle x_{un}(N)\rangle = -\frac{p_{tr}(N)\langle x_{tr}(N)\rangle}{p_{un}(N)} \tag{36}$$

where $p_{tr}(N)$ and $p_{un}(N)$ are the probabilities of being trapped and untrapped, respectively, by the Nth step, and $\langle x(N)\rangle$ are the corresponding displacements of the trapped and untrapped walks.

To compute these quantities, we appeal to a physical picture in which the random walk motion parallel and perpendicular to the needle are treated separately (figure 5). We first exploit this construction to compute the time dependence of the trapping probability. In two dimensions, when $x<0$, then the motion in the y direction is that of a one-dimensional random walk with a trapping point at $y=0$. This would yield a survival probability after n steps which decays as $n^{-1/2}$. However, when $x>0$, there is no trapping. The time intervals over which the walk is in the regions $x>0$, and $x<0$ grow as $n^{1/2}$. Accordingly, a plot of the survival probability on a double logarithmic scale would exhibit an alternating sequence of inclined intervals of slope $-\frac{1}{2}$, when $x<0$, and intervals of slope 0, when $x>0$. On a logarithmic scale, these intervals have approximately the same length. This implies that the survival probability, $p_{un}(n)$, decays as $n^{-1/4}$ (figure 6). In three dimensions, this same argument leads to $p_{un}(n)$ decaying at the same rate as that of a random walk with an excluded point in two dimensions, i.e. as $1/\ln n$, except that the amplitudes in the two problems are different.

We now use these results for the survival probability to compute the mean displacement of the untrapped walks. In two dimensions, $p_{un}(n)$ decaying as $n^{-1/4}$ implies that $p_{tr}(n)$, the probability of being trapped by the nth step, approaches unity as

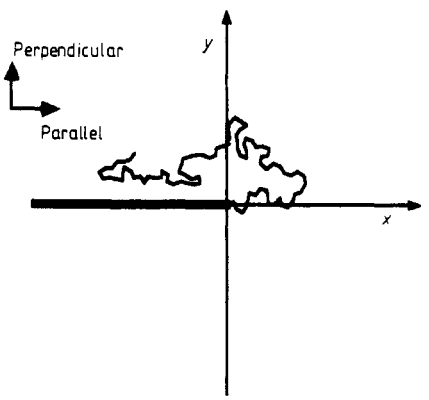

Figure 5. Schematic illustration of the decomposition of random walk motion into components parallel and perpendicular to the axis of the needle. Perpendicular to the axis, the motion is that of a $(d-1)$-dimensional random walk with an excluded point at the origin, when $x<0$.

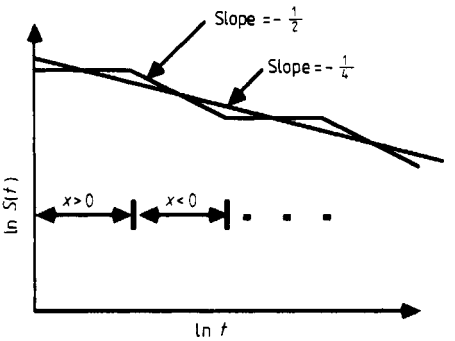

Figure 6. A double logarithmic plot of the expected behaviour of the survival probability for a two-dimensional random walk in the presence of an excluded needle. The average slope of the composite behaviour is $-1/4$.

$1-n^{-1/4}$. Thus the probability of being trapped at the nth step, $q(n)=\partial p_{\rm tr}(n)/\partial n \sim n^{-5/4}$. Consequently,

$$-\langle x_{\rm tr}(N)\rangle = \sum_{n}^{N} (\text{probability of hitting line at step } n) \times (\text{displacement at step } n)$$

$$\sim \sum_{n} n^{-5/4} n^{1/2} \sim N^{1/4}. \tag{37}$$

This leads to

$$\langle x_{\rm un}(N)\rangle \simeq (1-N^{-1/4})N^{1/4}N^{1/4} \sim N^{1/2}. \tag{38}$$

Similarly, in three dimensions, $p_{\rm un}(n)$ decaying as $1/\ln n$ implies that $p_{\rm tr}(n) \sim 1-1/\ln n$, leading to $q(n) \sim 1/(n(\ln n)^2)$. This then yields

$$\langle x_{\rm tr}(N)\rangle \simeq \sum_{n}^{N} \frac{1}{n(\ln n)^2} n^{1/2} \sim \frac{N^{1/2}}{(\ln N)^2}. \tag{39}$$

Finally, for $\langle x_{\rm un}(N)\rangle$, we obtain

$$\langle x_{\rm un}(N)\rangle \simeq \frac{N^{1/2}}{\ln N}. \tag{40}$$

It is very instructive to compare these asymptotic results with numerical data based on computing the exact probability distribution and mean displacement for a random walk in the presence of the excluded line. From these data, we calculate the finite-N approximants, ν_N, which describe the divergence of $\langle x_N\rangle$, by taking the slope of the line that joins $\langle x_N\rangle$ and $\langle x_{N+2}\rangle$ on a double logarithmic scale. Upon plotting the ν_N against $1/N$, it appears that the ν_N extrapolate to a value of approximately 0.55 for $N \leqslant 25$, and it is only for larger values of N that an unambiguous crossover to the asymptotic value of $\nu_{N\to\infty}=\frac{1}{2}$ is seen (figure 7(a)). In three dimensions, the values of ν_N appear to extrapolate to a value close to 0.365 for $N \leqslant 100$ when plotted against $1/N$. However, at the largest values of N, there is a small upward curvature to the data, which is indicative of a logarithmic correction (figure 7(b)). In fact, for the sequence $y_N = N^{1/2}/\ln N$, the $\nu_N \sim \frac{1}{2} - (1/\ln N) + \ldots$, and a plot of ν_N against $1/N$ would very slowly approach the asymptotic value of $\frac{1}{2}$ with an infinite slope. This behaviour closely mirrors what is observed in the RW data. Thus in both the two- and three-dimensional problems there is a very slow crossover to the asymptotic behaviour.

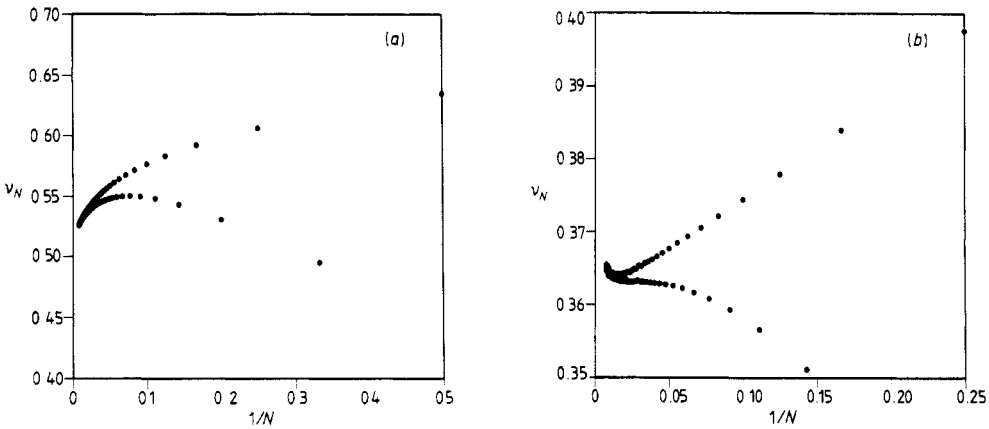

Figure 7. A plot of the exponent ν_N against $1/N$ for random walks in the presence of an excluded needle in (*a*) two dimensions and (*b*) three dimensions.

6. Discussion

In summary, we have studied the repulsion effects of excluding either a single point, or a half-line, on the asymptotic behaviour of the distribution of endpoint displacements of random and self-avoiding walks, as a function of the spatial dimension. In three and higher dimensions, the repulsion effect due to excluding a single lattice point is relatively weak. The first moment of the displacement converges to a finite value at a power-law rate, while the higher odd moments, $\langle x_N^{2k+1}\rangle$ scale as $N^{2k\nu}$.

The disappearance of the repulsion effect arising from an excluded site in three and higher dimensions motivated us to consider the general question of what is the minimal initial bias necessary to give rise to long-range repulsion, i.e. a diverging first moment, for random and/or self-avoiding walks as a function of the spatial dimension. To begin to address this general question, we investigated the repulsion effect of an excluded half-line, or needle. For SAWs in the presence of this excluded set, exact enumeration data indicate that $\langle x_N\rangle \sim N^{\nu}$, and that $\langle x_N^{2k+1}\rangle \sim N^{(2k+1)\nu}$, in two dimensions. However, in three dimensions, the available numerical data suggest that $\langle x_N^{2k+1}\rangle$ diverges $N^{z+2k\nu}$, where a new exponent, $z \simeq 0.35$, is apparently needed to characterise the distribution of endpoint displacements.

In order to help interpret this puzzling result, we also investigated the repulsion of random walks to the presence of an excluded needle and, more generally, the repulsion of random walks within an absorbing cone of opening angle θ_0, for which the excluded needle problem obtains in the limit $\theta_0 \to 2\pi$. The solution to the diffusion equation for this geometry indicates that the mean axial displacement away from the tip of the cone increases as $t^{1/2}$, independent of θ_0, even though the survival probability depends on the spatial dimension, and on θ_0. In three dimensions, however, the amplitude of $\langle x(t)\rangle$ vanishes as $\theta_0 \to 2\pi$, and the continuum approach does not easily yield the form of $\langle x(t)\rangle$ in the excluded needle limit. However, for this case heuristic arguments suggest that $\langle x_N\rangle \sim N^{1/2}/\ln N$ for discrete random walks.

The corresponding numerical data for $\langle x_N\rangle$ are consistent with these theoretical predictions. However, indications of asymptotic behaviour are not evident until relatively large values of N. This slow crossover possibly stems from the relatively large spatial region that the random walk must explore before the extent of the excluded

set is ascertained. This crossover may also be the source of our unusual results for SAWs in three dimensions. Indeed, within a mean-field approximation, the number of contacts of an N-step SAW with a semi-infinite line is *finite* as $N \to \infty$. This would suggest that $\langle x_N \rangle$ should also reach a finite limit as $N \to \infty$. This argument may be too crude, however, as the number of contacts of an N-step random walk with a semi-infinite line diverges as $\ln N$, and this small degree of repulsion appears to give rise to $\langle x_N \rangle$ diverging as $N^{1/2}/\ln N$. Owing to this sensitivity of displacement on the degree of repulsion, we cannot definitively exclude the possibility that $\langle x_N \rangle$ diverges for three-dimensional SAWs in the presence of an excluded needle.

Our results also raise the general question of the nature of the repulsion of a walk which starts at the tip of a d'-dimensional half-hyperplane embedded in a d-dimensional space. A natural expectation is that this general phenomenon would be characterised only by the codimension, $d - d'$, of the excluded set with respect to the embedding space. The extent to which this expectation does not hold in our studies suggests that the mechanism underlying the repulsion for half-hyperplane perturbations deserves further study. It may also prove to be fruitful to investigate the repulsion due to excluded sets of finite extent. For example, the excluded point and the excluded needle problem can be regarded as the extreme limits of an excluded finite-length needle problem in which the needle length goes to 0 or ∞, respectively. New insights into the general nature of the repulsion may be gained by investigating the crossover effects in this more general model.

Acknowledgments

We thank V Privman and T Witten for helpful discussions. The Center for Polymer Studies is supported in part by grants from the ARO, NSF and ONR. This financial support is gratefully acknowledged.

References

[1] Weiss G H 1981 *J. Math. Phys.* **22** 562
[2] Redner S and Privman V 1987 *J. Phys. A: Math. Gen.* **20** L857
[3] Montroll E W 1964 *Proc. Symp. Appl. Math.* **16** 193
[4] Montroll E W and Weiss G H 1965 *J. Math. Phys.* **6** 167
[5] Weiss G H and Rubin R J 1983 *Adv. Chem. Phys.* **52** 363
[6] Grassberger P 1982 *Phys. Lett.* **89A** 381
[7] Meirovitch H 1983 *J. Chem. Phys.* **79** 502
[8] Martin J L 1974 *Phase Transitions and Critical Phenomena* vol 2, ed C Domb and M S Green (New York: Academic)
[9] Redner S 1982 *J. Stat. Phys.* **29** 309
[10] Domb C and Fisher M E 1958 *Proc. Camb. Phil. Soc.* **54** 48
[11] Lindenberg K, Seshadri V, Shuler K E and Weiss G H 1980 *J. Stat. Phys.* **23** 11
[12] Carslaw H S and Jaeger J C 1959 *Conduction of Heat in Solids* (Oxford: Oxford University Press) p 458
[13] Ozisik M N 1980 *Heat Conduction* (New York: Wiley)
[14] Schulman L S 1982 *Phys. Rev. Lett.* **49** 599
[15] Hall R N 1949 *J. Appl. Phys.* **20** 925
[16] Schelkunoff S A 1941 *Proc. IRE* **29** 493